Fall 8-2015

An estimate of the second-order in-plane acceleration sensitivity of a Y-cut Quartz thickness-shear resonator

Huijing He
University of Nebraska - Lincoln, he.hui.jing@hotmail.com

Jiashi Yang
University of Nebraska - Lincoln

John A. Kosinski
MacAulay-Brown Inc.

An Estimate of the Second-Order In-Plane Acceleration Sensitivity of a Y-Cut Quartz Thickness-Shear Resonator

Huijing He, Jiashi Yang, and John A. Kosinski

***Abstract*—We perform a theoretical analysis of the second-order in-plane acceleration sensitivity of a Y-cut quartz thickness-shear mode resonator. The second-order nonlinear theory of elasticity for anisotropic crystals is used to determine the biasing fields in the resonator under in-plane acceleration. The acceleration-induced frequency shift is determined from a perturbation analysis based on the plate equations for small-amplitude vibrations superposed on a finite bias. We show that, whereas the first-order acceleration-induced frequency shift is zero for a structurally symmetric resonator under in-plane acceleration, the second-order frequency shift is nonzero and is quadratic in the acceleration. As the fourth-order nonlinear elastic constants of quartz have never been measured, we can only estimate the magnitude of the second-order frequency shift. For a particular case of interest, we find $\Delta\omega/\omega_0 \sim 10^{-18}$, 10^{-16}, and 10^{-14} when the acceleration is 1, 10, and 100 g, respectively.**

I. Introduction

Crystal resonators are essential components in modern military electronic systems used for surveillance, communication, and navigation in both airborne and vehicular applications. The performance of such systems often is bounded by limits imposed by the frequency stability of the crystal resonators used in critical reference circuits. For applications on mobile platforms such as helicopters, missiles, and satellites, any accelerations of the platform are transferred to the crystal resonators via their mounting structures and the forces involved induce initial (or biasing) deformations in the resonators that cause their resonant frequencies to shift [1], [2]. This phenomenon is known as resonator acceleration sensitivity, and it has remained an important research topic for many years. Well-known theoretical analyses were performed beginning in the late 1970s by Lee and coworkers [3]–[5] and continuing into the early 1990s by Tiersten and coworkers [6]–[9]. During this period a benchmark review of the phenomenology was published by Filler [10] followed by a pair of papers from Kosinski and coworkers providing detailed guidance for low acceleration sensitivity resonator design [11], [12]. Reported experimental results for the in-plane acceleration sensitivities of BAW and SAW quartz resonators and Y-cut langasite BAW resonators are listed in Table I. The results cover a variety of device types and mounting structures and the observed in-plane acceleration sensitivities range from values on the order of $10^{-9}/g$ for the oldest results down to on the order of $10^{-12}/g$ for the most recent results. This reflects both progress in understanding the structural mechanics nature of the problem and the creativity of designers in subsequently addressing the problem through improved mounting and isolation structures and the addition of electronic compensation circuits. Note that in virtually all cases, the listed in-plane acceleration sensitivities are substantially smaller than the corresponding normal acceleration sensitivities [13]–[35].

The basic effects of external accelerations on resonator frequencies can be described using a perturbation integral formulation [36] derived by Tiersten from the theory of small fields superposed on a bias in a crystal resonator [37]. This approach has been widely used to calculate acceleration-induced frequency shifts in various types of bulk acoustic wave and surface acoustic wave resonators. However, almost all of these theoretical results use only the first-order perturbation, which was assumed to be sufficient for the case of small accelerations on the order of 1 g. Not surprisingly, analyses using the first-order perturbation obtain a linear relationship between the acceleration and the resonator frequency shift. Of note, for perfectly symmetric resonators analyzed using thin-plate theory presuming an invariant plate thickness, the acceleration-induced frequency shift calculated using the first-order perturbation is zero for both normal and in-plane accelerations. This seemingly favorable result of "inherently zero" is mathematically correct but misleading because it arises only from the presumption of an invariant plate thickness that cannot be achieved in practice as the ever-present but nonlinear Poisson's effect is not considered. Present design and manufacturing capability can produce a limited yield of resonators with resonator-level acceleration sensitivity as small as $10^{-11}/g$ with $10^{-10}/g$ more typical. Over the past decade, the integration of active compensation schemes into oscillator electronics has yielded producible oscillator-level acceleration sensitivity as low as $10^{-12}/g$. It remains of interest to achieve such performance at the resonator level without the need for compensation electronics.

Manuscript received February 20, 2015; accepted June 4, 2015. This work was supported in part by the US Army Research Laboratory/US Army Research Office under agreement number W911NF-10-1-0293.

H. He and J. Yang are with the Department of Mechanical and Materials Engineering, University of Nebraska–Lincoln, Lincoln, NE 68588-0526, USA.

J. A. Kosinski is with the Advanced Technology Group, MacAulay-Brown Inc., Dayton, OH 45430, USA (e-mail: j.a.kosinski@ieee.org).

DOI http://dx.doi.org/10.1109/TUFFC.2015.007033

TABLE I. REPORTED VALUES FOR IN-PLANE ACCELERATION SENSITIVITIES OF QUARTZ AND LANGASITE BAW AND SAW RESONATORS.

Resonator (quartz and BAW except as noted)	In-plane acceleration sensitivity ($\times 10^{-10}/g$)	Acceleration level	Ref.
AT-cut 5.115 MHz fundamental	6 to 24	16 g peak sinusoidal at discrete frequencies across the range 100 to 2000 Hz	[13]
AT-cut 6.2 MHz fundamental	8 to 19	See above	[13]
SC-cut 5.115 MHz fundamental	6 to 9	See above	[13]
ST-cut 794 MHz SAW	130	10^{-2} to 10^{3} g peak	[14]
SC-cut 333 MHz fundamental	5.5 to 12.8	10 g peak	[15]
Rotated Y-cut 402 MHz SAW	Less than 2	10 g peak	[16]
ST-cut 402 MHz SAW	Less than 2	10 g peak implied	[17]
ST-cut 900 MHz SAW	Less than 2	10 g peak implied	[17]
AT-cut 40 MHz 5th OT	2.7 to 17	1 g rms	[18]
SC-cut 50 MHz 3rd OT	4.4 to 8.1	1 g rms	[18]
SC-cut 40 MHz 3rd OT	4.0 to 13	1 g rms	[18]
AT-cut 30 MHz 3rd OT	4.87 to 13.81 initial	5 g pk	[19]
AT-cut 30 MHz 3rd OT	0.95 to 2.26 adjusted	5 g pk	[19]
ST-cut 809 MHz SAW	30 to 200	2 g peak to peak	[20]
SAW delay line	10 to 500	Not specified	[21]
SAW resonator	12 to 60	Not specified	[21]
ST-cut 700 MHz to 1 GHz SAW	Less than 5	3 g peak	[22]
AT-cut 40 MHz 5th OT	18.8 to 23.4	Not specified	[23], [24]
SC-cut 40 MHz 3rd OT	3.8 to 7.6	Not specified	[23], [24]
ST-cut various 225 to 1403 MHz SAW	1.06 to 223	Sinusoidal 2 g	[25], [26]
320 MHz SAW	7 to 70	Not specified	[27], [28]
SC-cut 8 to 13 MHz	2.1 to 4.4	Not specified	[29]
SC-cut 100 MHz 3rd OT	1.2 to 7.2	1 g PSD random vibration at 0.0005 g^2/Hz over 5 to 2000 Hz	[30]
BVA-type	Less than 1.5	2 g peak to peak and random at unspecified level over 20 to 100 Hz	[31]
AT-cut 16.384 MHz rectangular	1 to 2	Sinusoidal 10 g peak at 70 Hz	[32]
SC-cut quad relief mount (QRM) plano-convex 10 MHz 3rd OT	0.29 to 23.1	Sinusoidal 10 g peak at 70 Hz	[33]
SC-cut QRM plano-convex 10 MHz 3rd OT	0.54 to 1.74	Not specified	[34]
Langasite Y-cut 10 MHz 3rd OT	0.98 to 1.78	Sinusoidal 10 g peak at 70 Hz	[35]

Resonators employed in military applications may experience acceleration levels on the order of hundreds of g. Experimental data obtained for resonator frequency shifts under large acceleration exhibit a nonlinear dependence on the acceleration level [38], and the case of large external acceleration clearly requires a higher-order perturbation analysis. Such is also true for the case of small external accelerations applied to symmetric structures where the magnitudes of any first-order perturbations are expected to be at or near zero. For example, it has been shown that, for the normal acceleration sensitivity of perfectly symmetric resonators, although the first-order effects of the acceleration do not produce any frequency shift, the second-order effects of the acceleration result in a nonzero lower bound on the normal acceleration sensitivity [39]–[42] on the order of $10^{-11}/g$. Therefore, analyses aimed at guiding the reduction of acceleration sensitivity to the level of $10^{-12}/g$ must necessarily include second-order effects.

Proper calculation of higher-order perturbations is contingent upon knowledge of complete sets of higher-order material constants through the fourth order. Whereas the fourth-order effective elastic stiffness $\tilde{c}_{6666}$ has been reported for the AT-cut [43]–[46], complete sets of fundamental fourth-order material constants are not available [47], and as a result it is only possible to estimate the order of magnitude of the effects. We note that, in general, the gross magnitudes of the elastic constants grow by one order of magnitude as the rank increases [c(3) ~10 c(2), and c(4) ~100 c(2)]. Although there are some estimates of the second-order normal acceleration sensitivity of crystal resonators [39]–[42], there are no reported theoretical results on the second-order in-plane acceleration sensitivity. In this paper we try to estimate this effect through a theoretical analysis. In particular, we are concerned with whether the second-order in-plane acceleration sensitivity of a perfectly symmetric resonator is zero or not, and if not, determining its order of magnitude.

II. NONLINEAR EXTENSION OF A RESONATOR UNDER IN-PLANE ACCELERATION

In this section we obtain the nonlinear extension of a quartz plate resonator under in-plane acceleration including second-order effects. To capture the second-order effects of the acceleration-induced biasing fields, we need the nonlinear theory for electroelastic solids as in [48]. Quartz has very weak piezoelectric coupling. For the frequency analysis, we neglect the small piezoelectric coupling included in [48]; [48] in fact also includes third-order nonlinear effects that are not needed for the purpose of the present paper limited to second-order effects. Let the

deformation of the body be described by $y_i = \delta_{iL}(X_L + U_L)$, where y_i and X_L denote the present and reference coordinates of material points. δ_{jM} is the Kronecker delta. Our notation here differs from [48] in that we use a capital U_L for the displacement vector because the lowercase u needs to be saved for later use in the equations from another important reference [49] of the present paper. The equations of motion are [48]

$$K_{Lj,L} + \rho_0 f_j = \rho_0 \ddot{U}_j, \tag{1}$$

where ρ_0 is the mass density, f_j is the body force, K_{Lk} is the first Piola-Kirchhoff stress tensor, and $U_j = \delta_{jL}U_L$. A superimposed dot represents time derivative. For a theory including all second-order effects of the displacement gradient $U_{K,L}$, we have [48]

$$\begin{aligned} K_{LM} = {} & c_{LMAB}U_{A,B} + \frac{1}{2}c_{LMAB}U_{N,A}U_{N,B} \\ & + \frac{1}{2}c_{LMABCD}U_{A,B}U_{C,D} + c_{KLAB}U_{A,B}U_{M,K}, \end{aligned} \tag{2}$$

where c_{ABCD} and c_{ABCDEF} are the second- and third-order elastic constants, and we have denoted $K_{LM} = K_{Lj}\delta_{jM}$, which is asymmetric in general.

Consider the plate in Fig. 1 with a normal along X_2. The plate is assumed to be thin, for which we have the following stress relaxation [50]:

$$K_{21} = 0, \quad K_{22} = 0, \quad K_{23} = 0, \tag{3}$$

or, with the use of (2),

$$\begin{aligned} & c_{21AB}U_{A,B} + \frac{1}{2}c_{21AB}U_{N,A}U_{N,B} + \frac{1}{2}c_{21ABCD}U_{A,B}U_{C,D} \\ & \quad + \; c_{K2AB}U_{A,B}U_{1,K} = 0, \\ & c_{22AB}U_{A,B} + \frac{1}{2}c_{22AB}U_{N,A}U_{N,B} + \frac{1}{2}c_{22ABCD}U_{A,B}U_{C,D} \\ & \quad + \; c_{K2AB}U_{A,B}U_{2,K} = 0, \\ & c_{23AB}U_{A,B} + \frac{1}{2}c_{23A,B}U_{N,A}U_{N,B} + \frac{1}{2}c_{23ABCD}U_{A,B}U_{C,D} \\ & \quad + \; c_{K2AB}U_{A,B}U_{3,K} = 0. \end{aligned} \tag{4}$$

We need to solve (4) for $U_{2,1}$, $U_{2,2}$, $U_{2,3}$. They are present in both of the linear and nonlinear terms of (4). We solve (4) approximately by an iteration procedure [51]. As the first step of the iteration, we solve the linear part of (4) for $U_{2,1}$, $U_{2,2}$, $U_{2,3}$. We then substitute the linear solutions of $U_{2,1}$, $U_{2,2}$, $U_{2,3}$ into the nonlinear terms in (4) and solve the resulting equations again for $U_{2,1}$, $U_{2,2}$, $U_{2,3}$ as the second iteration. The solutions of $U_{2,1}$, $U_{2,2}$, $U_{2,3}$ from the second iteration are then substituted into the expressions for K_{11}, K_{13}, K_{31}, and K_{33} in (2). The resulting expressions for K_{11}, K_{13}, K_{31}, and K_{33} do not depend on $U_{2,1}$, $U_{2,2}$, $U_{2,3}$ and are ready to be used for describing the extension of thin plates. For extension, following the notation of [49], we approximate the displacement field by

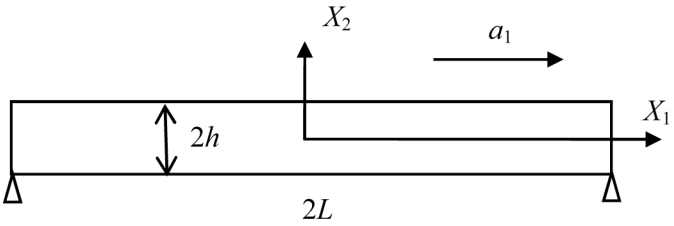

Fig. 1. A crystal plate under in-plane acceleration a_1 directed along the X_1-axis (X_3 is determined from X_1 and X_2 by the right-hand rule).

$$\begin{aligned} & U_1 \cong U_1^{(0)}(X_1, X_3, t), \quad U_2 \cong X_2 U_2^{(1)}(X_1, X_3, t), \\ & U_3 \cong U_3^{(0)}(X_1, X_3, t), \end{aligned} \tag{5}$$

which yields the following expressions for the remaining components of the displacement gradient:

$$\begin{aligned} & U_{1,1} = U_{1,1}^{(0)}, \quad U_{1,2} = 0, \quad U_{1,3} = U_{1,3}^{(0)}, \\ & U_{3,1} = U_{3,1}^{(0)}, \quad U_{3,2} = 0, \quad U_{3,3} = U_{3,3}^{(0)}. \end{aligned} \tag{6}$$

The equations for extension to be developed are two-dimensional equations governing $U_1^{(0)}$ and $U_3^{(0)}$. The $U_2^{(1)}$ in (5) is eliminated from the stress relaxation procedure discussed above. The equations of motion for extension are obtained by integrating (1) for $j = 1$ and 3 through the plate thickness:

$$K_{BA,B}^{(0)} + \rho_0 f_j 2h = 2\rho_0 h \ddot{u}_A^{(0)}, \quad A, B = 1, 3, \tag{7}$$

where the plate resultants for extensional motions are defined by

$$K_{BA}^{(0)} = \int_{-h}^{h} K_{BA} \mathrm{d}X_2, \tag{8}$$

which depends on $U_1^{(0)}$ and $U_3^{(0)}$ only. Substitution of (8) into (7) gives the two equations for $U_1^{(0)}$ and $U_3^{(0)}$ describing extension.

For an estimate of the in-plane acceleration sensitivity of the plate in Fig. 1, it is sufficient to consider the one-dimensional case without dependence on X_3, and $U_3^{(0)} = 0$. We have the following boundary-value problem for the extensional deformation due to the in-plane acceleration a_1 in Fig. 1:

$$\begin{aligned} & K_{11,1}^{(0)} + \rho_0(-a_1)2h = 0, \quad |X_1| < L, \\ & U_1^{(0)} = 0, \quad X_1 = \pm L, \end{aligned} \tag{9}$$

where the relevant extensional resultant is given by

$$K_{11}^{(0)} = 2h[\beta_1 U_{1,1}^{(0)} + \beta_2 (U_{1,1}^{(0)})^2]. \tag{10}$$

β_1 and β_2 are functions of the second- and third-order elastic constants. Their expressions are lengthy (see Appendix). In the special case when $\beta_2 = 0$, (10) becomes linear. Similar to what was done in the inversion of the stress relaxation conditions above, through an iteration proce-

dure based on the linear solution of $(9)_1$, an approximate solution to $(9)_1$ quadratically nonlinear in a_1 is found to be

$$U_1 = -\frac{\beta_2\rho_0^2 a_1^2 X_1^3}{3\beta_1^3} + \left(\frac{\rho_0 a_1}{2\beta_1} - \frac{\alpha_2\rho_0 a_1 E}{\beta_1^3}\right)X_1^2 + \left(\frac{E}{\beta_1} - \frac{\beta_2 E^2}{\beta_1^3}\right)X_1 + F, \tag{11}$$

where E and F are integration constants determined by the boundary conditions in $(9)_2$. When $\beta_2 = 0$ and $E = 0$, (11) reduces to the linear solution. For some insight, an approximate expression for E accurate to the second-order of a_1 can be found from an iteration procedure as

$$E = \frac{1}{3}\frac{\beta_2}{\beta_1^2}\rho_0^2 L^2 (a_1)^2, \tag{12}$$

which is a pure second-order effect without a term linear in a_1. Then the a_1E and E^2 terms in (11) are in fact negligible.

In Fig. 2(a) we plot the distribution of $U_{1,1}$ along X_1 for different values of in-plane acceleration a_1 directed along the X_1-axis. A Y-cut quartz resonator is assumed because the second- and third-order elastic constants are directly available. Physically $U_{1,1}$ is related to the extensional strain along X_1. In the figure, a larger acceleration produces a larger strain distribution as expected. Due to the symmetry of the plate in X_1 and the in-plane acceleration which is effectively an antisymmetric load, the linear solution for $U_{1,1}$ is exactly a straight line odd in X_1, describing the fact that the right half of the plate is in tension with a positive $U_{1,1}$ and the left half is in compression with a negative $U_{1,1}$. However, a magnification of Fig. 2(a) near the origin as seen in Fig. 2(b) shows that the curves do not pass through the origin as would be the case for the corresponding first-order (linear) solution. In other words, the nonlinear solution does not possess the symmetry or antisymmetry of the corresponding linear solution. Similarly, Fig. 3 shows the distribution of $U_{2,2}$ along X_1 for different values of a_1, which is determined from the stress relaxation conditions. When the right half of the plate is in extension, it becomes thinner as represented by a negative $U_{2,2}$ in the figure due to the well-known Poisson's effect. Again the curves do not go through the origin, indicating a loss of symmetry. This loss of symmetry or antisymmetry has important implications for the second-order resonator frequency shift to be calculated in the next section.

III. Second-Order In-Plane Acceleration Sensitivity

With the acceleration-induced biasing deformation determined in the previous section, we are ready to study the crystal plate in thickness-shear vibration superposed on the biasing extensional deformation. Let the thickness-shear motion be described by $u_1 \cong X_2 u_1^{(1)}(X_1, t)$, $u_2 \cong 0$, and $u_3 \cong 0$. Then $u_1^{(1)}$ is governed by (see $(59)_2$ of [49]):

$$\begin{aligned}
&[(1 + U_{1,1}^{(0)})t_1^{(1)}]_{,1} - (1 + U_{1,1}^{(0)})t_6^{(0)} = \frac{2}{3}h^3\rho_0\ddot{u}_1^{(1)}, \quad |X_1| < L,\\
&u_1^{(1)} = 0, \quad X_1 = \pm L,
\end{aligned} \tag{13}$$

where [44]

$$\begin{aligned}
t_6^{(0)} &= 2h\kappa^2(c_{66} + c_{661}E_1^{(0)} + c_{662}E_2^{(0)})(1 + U_{1,1}^{(0)})u_1^{(1)},\\
t_1^{(1)} &= \frac{2h^3}{3}(c_{11} + c_{111}E_1^{(0)} + c_{112}E_2^{(0)})(1 + U_{1,1}^{(0)})u_{1,1}^{(1)},\\
E_1^{(0)} &= U_{1,1}^{(0)} + \frac{1}{2}(U_{1,1}^{(0)})^2,\\
E_2^{(0)} &= U_2^{(1)} + \frac{1}{2}[(U_{1,1}^{(0)})^2 + (U_2^{(1)})^2],\\
\kappa^2 &= \frac{\pi^2}{12}.
\end{aligned} \tag{14}$$

Substituting (14) into $(13)_1$, keeping up to the second-order effects of $U_{1,1}^{(0)}$, for free vibrations with a frequency ω, we obtain the following equation for $u_1^{(1)}$:

$$\begin{aligned}
&\frac{2}{3}h^3[(c_{11} + \Delta c_{11})u_{1,1}^{(1)}]_{,1} - 2h\kappa^2(c_{66} + \Delta c_{66})u_1^{(1)}\\
&\quad = -\frac{2}{3}h^3\rho\omega^2 u_1^{(1)},
\end{aligned} \tag{15}$$

where

$$\begin{aligned}
\Delta c_{11} &= \delta_1 U_{1,1}^{(0)} + \delta_2\left[U_{1,1}^{(0)}\right]^2,\\
\Delta c_{66} &= \delta_3 U_{1,1}^{(0)} + \delta_4\left[U_{1,1}^{(0)}\right]^2.
\end{aligned} \tag{16}$$

δ_1 through δ_4 are complicated functions of the second- and third-order elastic constants. We solve (15) with the boundary conditions in $(13)_2$ using a perturbation procedure. The zero-order problem of the procedure is when the acceleration and the biasing field $U_1^{(0)} = 0$. We denote the frequency and mode in this case by ω_0 and u. They are governed by

$$\begin{aligned}
&\frac{2}{3}h^3(c_{11}u_{,1})_{,1} - 2h\kappa^2 c_{66}u = -\frac{2}{3}h^3\rho\omega_0^2 u, \quad |X_1| < L,\\
&u = 0, \quad X_1 = \pm L.
\end{aligned} \tag{17}$$

The eigenvalue problem in (17) has a series of solutions for its frequencies and the corresponding modes. For resonator applications, we are only interested in the following fundamental mode without any nodal points (zeros) along the X_1 axis:

$$\begin{aligned}
\omega_0 &= \sqrt{\frac{c_{11}}{\rho}\left(\frac{\pi}{2L}\right)^2 + \frac{3\kappa^2 c_{66}}{\rho h^2}},\\
u(X_1) &= C\cos\frac{\pi X_1}{2L},
\end{aligned} \tag{18}$$

where C is an arbitrary constant. For the first-order problem of the perturbation procedure we write

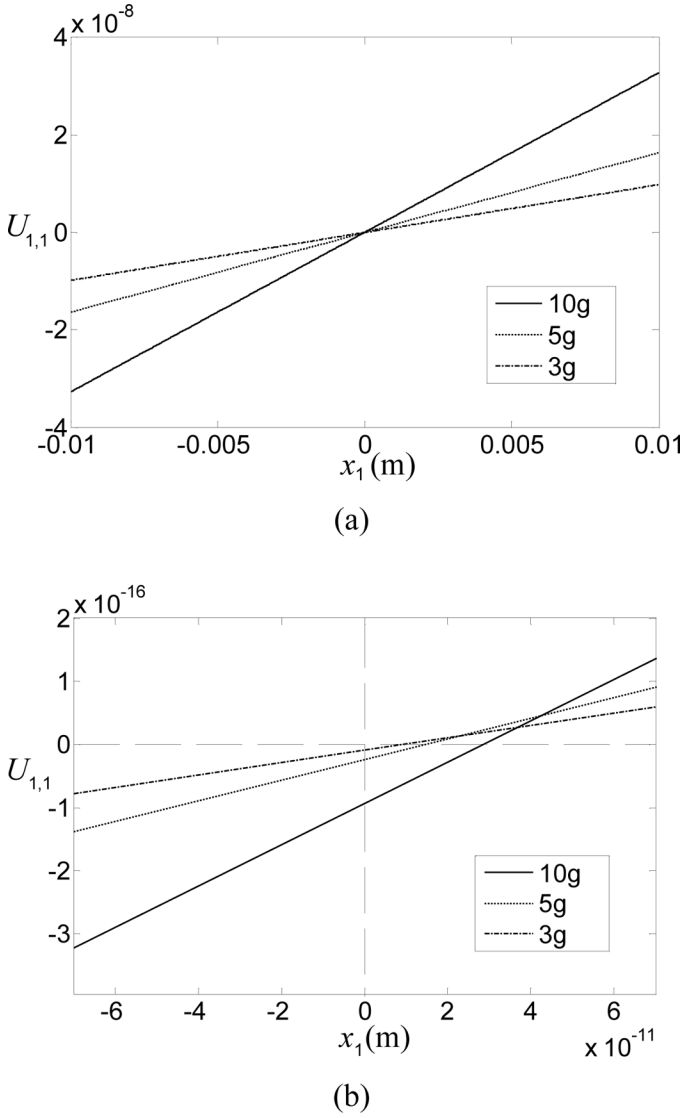

Fig. 2. Distribution of $U_{1,1}$. $L = 10$ mm. $h = 0.5$ mm. (a) Global view along the entire plate. (b) Local view near the center. Note the changes in both x- and y-axis scales between (a) and (b).

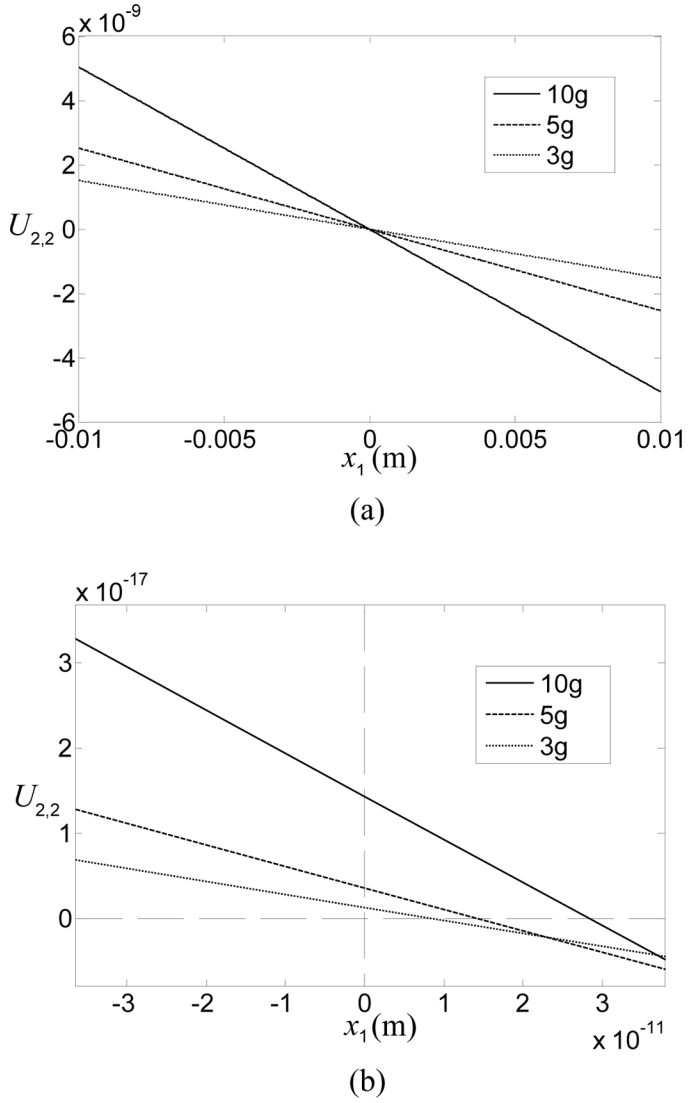

Fig. 3. Distribution of $U_{2,2}$. $L = 10$ mm. $h = 0.5$ mm. (a) Global view along the entire plate. (b) Local view near the center. Note the changes in both x- and y-axis scales between (a) and (b).

$$\begin{aligned} \omega &= \omega_0 + \Delta\omega, \\ u_1^{(1)} &= u + \Delta u, \end{aligned} \tag{19}$$

substitute them into (15), neglect the products of the terms associated with Δ, make use of (17), and obtain the following equations governing $\Delta\omega$ and Δu:

$$\begin{aligned} &\frac{1}{3}h^2(\Delta c_{11}u_{,1}+c_{11}\Delta u_{,1})_{,1}-\kappa^2(\Delta c_{66}u + c_{66}\Delta u) \\ &\quad = -\frac{1}{3}h^2\rho\left(2\omega_0\Delta\omega u + \Delta u\omega_0^2\right), \quad |X_1| < L, \\ &\Delta u = 0, \quad X_1 = \pm L. \end{aligned} \tag{20}$$

To solve (20) for $\Delta\omega$, we multiply both sides of $(20)_1$ by u, apply integration by parts to the first term on the left, and use (17). This leads to

$$\frac{\Delta\omega}{\omega_0} = \frac{\frac{h^2}{3}\int_{-L}^{L}\Delta c_{11}u_{,1}^2 \mathrm{d}X_1 + \kappa^2\int_{-L}^{L}\Delta c_{66}u^2\mathrm{d}X_1}{\frac{2}{3}\rho h^2\omega_0^2\int_{-L}^{L}u^2\mathrm{d}X_1}, \tag{21}$$

which includes the second-order effects of the biasing fields through (16). It can be seen from (21), (18), (16), and (11) that, for the linear effects of small accelerations, Δc_{11} and Δc_{66} are odd (linear) functions of X_1 whereas u^2 and $(u_{,1})^2$ are even functions of X_1. Therefore the linear acceleration sensitivity for the symmetric resonator we are considering is zero, as expected. However, when second-order effects need to be considered, the loss of symmetry due to second-order effects as shown in Figs. 2 and 3 makes the integration in the numerator of (21) nonzero.

In Fig. 4 we plot (21) for fixed L in (a) or fixed h in (b). For second-order effects, the curves are parabolic as expected. From the figure and the quadratic dependence of the frequency shift on the acceleration, the second-order

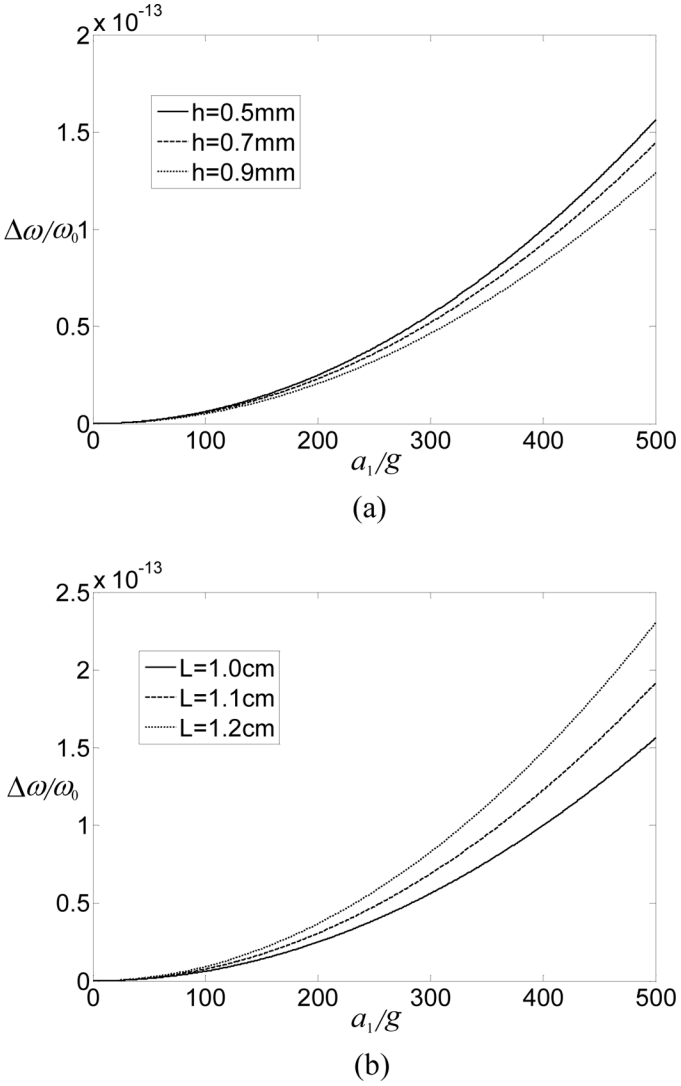

Fig. 4. Acceleration-induced frequency shift as the magnitude of the acceleration a_1 varies from 0 g up to 500 g. (a) Thickness h is varied as length L is held constant at $L = 10$ mm. (b) Length L is varied as thickness h is held constant at $h = 0.5$ mm.

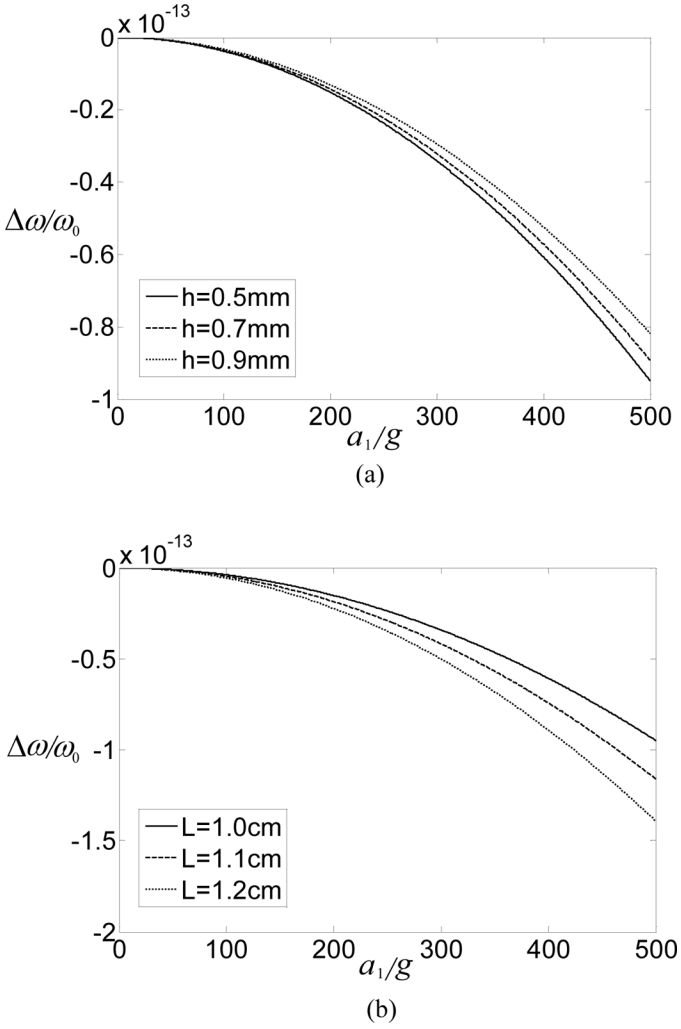

Fig. 5. Acceleration-induced frequency shift calculated with all third-order constants set to zero. The calculation is similar to that of Fig. 4 but limited strictly to the contribution arising from second-order material constants as the magnitude of the acceleration a_1 varies from 0 g up to 500 g. (a) Thickness h is varied as length L is held constant at $L = 10$ mm. (b) Length L is varied as thickness h is held constant at $h = 0.5$ mm.

frequency shift is roughly of the order of $\Delta\omega/\omega_0 = 10^{-18}$, 10^{-16}, and 10^{-14} when the acceleration is 1, 10, and 100 g, respectively. This is much smaller than the second-order normal acceleration sensitivity of the same device configuration which was estimated to be of the order of 10^{-11} per g in [39]–[42]. In the extreme case of guided cannon shells, which have the largest acceleration (2500 g) known to the authors, (21) gives a frequency shift of the order of 10^{-12} which may be relevant.

In 1987, J. J. Gagnepain pointed out, "The nonlinear behavior of piezoelectric devices is described not only by the nonlinear fundamental constants, but rather by effective constants which involve 2nd order, 3rd order, and sometimes 4th order fundamental constants. This means that a crystal with zero nonlinear fundamental constants—irrealistic hypothesis—would still exhibit nonlinear properties" [47]. This point is illustrated in Fig. 5 where the second-order frequency shift is plotted for the same acceleration but while setting all third-order material constants to zero. The magnitude of the contribution to the frequency shift from the second-order constants is nearly half that of the contribution to the frequency shift from third-order constants.

Finally, we point out that, for a complete description of the second-order effects of biasing fields, a second-order perturbation theory is needed [40], [52]. However, the second-order frequency perturbation integral requires the fourth-order elastic constants, which at present are unavailable. Therefore, in this paper, we limit our goal to giving an estimate of the order of magnitude of the second-order effect of in-plane accelerations.

IV. Conclusion

An estimate of the second-order in-plane acceleration sensitivity of a Y-cut quartz resonator has been obtained.

The acceleration-induced frequency shift depends quadratically on the acceleration and is nonzero for a structurally symmetric resonator. This imposes a nonzero lower bound on the in-plane acceleration sensitivity. For the device dimensions considered here, when the acceleration is 1, 10, and 100 g, the corresponding second-order frequency shift is of the order of $\Delta\omega/\omega_0 = 10^{-18}$, 10^{-16}, and 10^{-14}, respectively. These are smaller than the second-order normal acceleration sensitivity by a few orders of magnitude and are not of concern for the present technologies in general except in some extreme applications. In consequence, efforts on the reduction of second-order acceleration sensitivity should be directed toward reducing the second-order normal acceleration sensitivity.

Appendix
Equations for the Constants β_1 and β_2

$$P = \frac{c_{14}c_{24} - c_{12}c_{44}}{c_{22}c_{44} - c_{24}^2}, \tag{A1}$$

$$Q = \frac{c_{12}c_{24} - c_{22}c_{14}}{c_{22}c_{44} - c_{24}^2}U_{1,1}, \tag{A2}$$

$$A_1 = -c_{12}, \tag{A3}$$

$$\begin{aligned} B_1 = &-\frac{1}{2}(c_{12} + c_{112}) - \frac{1}{2}(3c_{22} + c_{222})P^2 \\ &- \frac{1}{2}(c_{23} + 2c_{44} + c_{244})Q^2 - (3c_{24} + c_{224})PQ \\ &- (c_{14} + c_{124})Q - (c_{12} + c_{122})P, \end{aligned} \tag{A4}$$

$$C_1 = -c_{14}, \tag{A5}$$

$$\begin{aligned} D_1 = &-\frac{1}{2}(c_{14} + c_{114}) - \frac{1}{2}(c_{24} + c_{224})P^2 - \frac{1}{2}(c_{34} + c_{444})Q^2 \\ &- (c_{44} + c_{244})PQ - c_{124}P - c_{144}Q, \end{aligned} \tag{A6}$$

$$A = \frac{c_{44}A_1 - c_{24}C_1}{c_{22}c_{44} - c_{24}^2}, \tag{A7}$$

$$B = \frac{c_{44}B_1 - c_{24}D_1}{c_{22}c_{44} - c_{24}^2}, \tag{A8}$$

$$C = \frac{c_{22}C_1 - c_{24}A_1}{c_{22}c_{44} - c_{24}^2}, \tag{A9}$$

$$D = \frac{c_{22}D_1 - c_{24}B_1}{c_{22}c_{44} - c_{24}^2}, \tag{A10}$$

$$\beta_1 = c_{11} + c_{12}A + c_{14}C, \tag{A11}$$

$$\begin{aligned} \beta_2 = &\frac{3}{2}c_{11} + \frac{1}{2}c_{111} + (c_{12} + c_{112})A + c_{12}B + (c_{14} + c_{114})C \\ &+ c_{14}D + \frac{1}{2}(c_{12} + c_{122})A^2 + \frac{1}{2}(c_{13} + c_{144})C^2 \\ &+ (c_{14} + c_{124})AC. \end{aligned} \tag{A12}$$

References

[1] A. Ballato, "Crystal resonators with increased immunity to acceleration fields," *IEEE Trans. Sonics Ultrason.*, vol. 27, no. 4, pp. 195–201, 1980.

[2] J. R. Vig, "Military applications of high accuracy frequency standards and clocks," *IEEE Trans. Ultrason. Ferroelectr. Freq. Control*, vol. 40, no. 5, pp. 522–527, 1993.

[3] P. C. Y. Lee, K. M. Wu, and Y. S. Wang, "Effects of acceleration on the resonance frequencies of crystal plates," *J. Acoust. Soc. Am.*, vol. 63, no. 4, pp. 1039–1047, 1978.

[4] P. C. Y. Lee and K. M. Wu, "In-plane accelerations and forces on frequency changes in doubly rotated quartz plates," *J. Acoust. Soc. Am.*, vol. 75, no. 4, pp. 1105–1117, 1984.

[5] P. C. Y. Lee and X. Guo, "Acceleration sensitivity of crystal resonators affected by the mass and location of electrodes," *IEEE Trans. Ultrason. Ferroelectr. Freq. Control*, vol. 38, no. 4, pp. 358–365, 1991.

[6] H. F. Tiersten and D. V. Shick, "On the normal acceleration sensitivity of ST-cut quartz surface wave resonators supported along rectangular edges," *J. Appl. Phys.*, vol. 64, no. 9, pp. 4334–4341, 1988.

[7] H. F. Tiersten and Y. S. Zhou, "On the in-plane acceleration sensitivity of contoured quartz resonators supported along rectangular edges," *J. Appl. Phys.*, vol. 70, no. 9, pp. 4708–4714, 1991.

[8] H. F. Tiersten and D. V. Shick, "On the normal acceleration sensitivity of contoured quartz resonators rigidly supported along rectangular edges," *J. Appl. Phys.*, vol. 67, no. 1, pp. 60–67, 1990.

[9] D. V. Shick, Y. S. Zhou, and H. F. Tiersten, "An analysis of the in-plane acceleration sensitivity of quartz surface wave resonators rigidly supported along the edges," *J. Appl. Phys.*, vol. 65, no. 1, pp. 35–40, 1989.

[10] R. L. Filler, "The acceleration sensitivity of quartz crystal oscillators: A review," *IEEE Trans. Ultrason. Ferroelectr. Freq. Control*, vol. 35, no. 3, pp. 297–305, 1988.

[11] J. A. Kosinski and A. Ballato, "Designing for low acceleration sensitivity," *IEEE Trans. Ultrason. Ferroelectr. Freq. Control*, vol. 40, no. 5, pp. 532–537, 1993.

[12] J. A. Kosinski and R. A. Pastore Jr., "Theory and design of piezoelectric resonators immune to acceleration: Present state of the art," *IEEE Trans. Ultrason. Ferroelectr. Freq. Control*, vol. 48, no. 5, pp. 1426–1437, 2001.

[13] R. L. Filler, L. J. Keres, T. M. Snowden, and J. R. Vig, "Ceramic flatpack enclosed AT and SC-cut resonators," in *Proc. IEEE Ultrasonics Symp.*, 1980, pp. 819–824.

[14] B. H. Kolner, "Microphonic sensitivity of surface acoustic wave resonators," *IEEE Trans. Ultrason. Ferroelectr. Freq. Control*, vol. 35, no. 3, pp. 365–371, May 1988.

[15] R. C. Smythe and R. B. Angove, "Chemically-milled UHF SC-cut resonators," in *Proc. 42nd Annu. Frequency Control Symp.*, 1988, pp. 73–77.

[16] J. A. Greer and T. E. Parker, "Improved vibration sensitivity of the All Quartz Package," in *Proc. 42nd Annu. Frequency Control Symp.*, 1988, pp. 239–251.

[17] T. E. Parker and G. K. Montress, "Frequency stability of high performance SAW oscillators," in *Proc. IEEE Ultrasonics Symp.*, 1989, pp. 37–45.

[18] M. M. Driscoll, "Quartz crystal resonator g-sensitivity measurement methods and recent results," in *Proc. 43rd Annu. Frequency Control Symp.*, 1989, pp. 419–426.

[19] R. C. Smythe and W. H. Horton, "Adjustment of resonator g-sensitivity by circuit means," in *Proc. 44th Annu. Symp. on Frequency Control*, 1990, pp. 437–443.

[20] A. Ballato, J. Kosinski, T. Lukaszek, M. Mizan, and R. McGowan, "Electronic desensitization of resonators to accelerations," in *Proc. 44th Annu. Symp. on Frequency Control*, 1990, pp. 444–451.

[21] J. Kosinski, A. Ballato, and T. Lukaszek, "Measurements of acceleration-induced phase noise in surface acoustic wave devices," in *Proc. 44th Annu. Symp. on Frequency Control*, 1990, pp. 488–492.

[22] T. E. Parker, J. A. Greer, and G. K. Montress, "SAW oscillators with low vibration sensitivity," in *Proc. 45th Ann. Symp. on Frequency Control*, 1991, pp. 321–329.

[23] M. M. Driscoll, "Reduction of quartz crystal oscillator flicker-of-frequency and white phase noise (floor) levels and acceleration sensitivity via use of multiple resonators," *IEEE Trans. Ultrason. Ferroelectr. Freq. Control*, vol. 40, no. 4, pp. 427–430, Jul. 1993.

[24] M. M. Driscoll, "Reduction of quartz crystal oscillator flicker-of-frequency and white phase noise (floor) levels and acceleration sensitivity via use of multiple resonators," in *IEEE Freq. Contr. Symp.*, 1992, pp. 334–339.
[25] R. McGowan, J. Himmel, J. Kosinski, R. Lindenmuth, and T. Lukaszek, "Acceleration sensitivity of SAW oscillators: A market survey," in *IEEE Ultrasonics Symp.*, 1992, pp. 207–210.
[26] R. McGowan, J. Kosinski, R. Lindenmuth, J. Himmel, and T. Lukaszek, "Acceleration sensitivity study for commercially available SAW oscillators," in *IEEE Microwave Symp. Dig.*, 1993, pp. 381–384.
[27] M. M. Driscoll, "A SAWR vibration sensitivity and phase noise reduction technique using multiple resonators and RF outputs," in *IEEE Ultrasonics Symp.*, 1994, pp. 37–41.
[28] M. M. Driscoll, "A SAWR vibration sensitivity and phase noise reduction technique using multiple resonators and RF outputs," in *IEEE Int. Frequency Control Symp.*, 1995, pp. 514–518.
[29] I. V. Abramson, "Internal heated quartz resonator with low sensitivity to an acceleration," in *IEEE Int. Frequency Control Symp.*, 1995, pp. 838–842.
[30] G. Labruzzo, P. Polidoro, M. Driscoll, and G. Kolnowski, "A VHF quartz crystal oscillator exhibiting exceptional vibration immunity," in *IEEE Int. Frequency Control Symp.*, 1996, pp. 473–480.
[31] J. J. Boy, F. Deyzac, and N. Gufflet, "BVA resonators: Analysis of its low g-sensitivity," in *IEEE Ultrasonics Symp.*, 1998, pp. 905–908.
[32] J. T. Stewart, P. Morley, and D. S. Stevens, "Theoretical and experimental results for the acceleration sensitivity of rectangular crystal resonators," in *Joint Meeting of the European Frequency and Time Forum and the IEEE Int. Frequency Control Symp.*, 1999, pp. 490–493.
[33] R. B. Haskell, P. E. Morley, and D. S. Stevens, "High Q, precision SC cut resonators with low acceleration sensitivity," in *IEEE Int. Freq. Contr. Symp. and Piezoelectric Devices Association Exhibition*, 2002, pp. 111–118.
[34] R. B. Haskell, J. E. Buchanan, P. E. Morley, B. B. Desai, M. A. Esmiol, M. E. Martin, and D. S. Stevens, "State-of-the-art in the design and manufacture of low acceleration sensitivity resonators," in *IEEE Int. Ultrasonics, Ferroelectrics, and Frequency Control Joint 50th Anniversary Conf.*, 2004, pp. 672–677.
[35] R. B. Haskell, J. E. Buchanan, B. B. Desai, D. S. Stevens, and Y. Kim, "Acceleration sensitivity measurements of quad relief mount langasite resonators," in *IEEE Int. Frequency Control Symp.*, 2008, pp. 237–239.
[36] H. F. Tiersten, "Perturbation theory for linear electroelastic equations for small fields superposed on a bias," *J. Acoust. Soc. Am.*, vol. 64, no. 3, pp. 832–837, 1978.
[37] J. C. Baumhauer and H. F. Tiersten, "Nonlinear electroelastic equations for small fields superposed on a bias," *J. Acoust. Soc. Am.*, vol. 54, no. 4, pp. 1017–1034, 1973.
[38] M. Nakazawa, T. Lukaszek, and A. Ballato, "Force- and acceleration-frequency effects in grooved and ring-supported resonators," in *Proc. IEEE Int. Frequency Control Symp.*, 1981, pp. 71–91.
[39] J. A. Kosinski, R. A. Pastore, Jr., and J. S. Yang, "Implications of in-plane stretch and thickness compression coupled to flexure on the lower bound of BAW acceleration sensitivity," in *Proc. IEEE Int. Frequency Control Symp.*, 2000, pp. 345–347.
[40] J. A. Kosinski, R. A. Pastore, J. S. Yang, X. M. Yang, and J. A. Turner, "Second-order frequency shifts in crystal resonators under relatively large biasing fields," in *Proc. IEEE Int. Frequency Control Symp.*, 2002, pp. 103–110.
[41] J. S. Yang and S. H. Guo, "An estimate on the second-order normal acceleration sensitivity of a quartz resonator," *IEEE Trans. Ultrason. Ferroelectr. Freq. Control*, vol. 53, no. 9, pp. 1562–1563, 2006.
[42] J. S. Yang and S. H. Guo, "Reduction of crystal resonator second order normal acceleration sensitivity by overhang plates," *Appl. Phys. Lett.*, vol. 88, no. 19, art. no. 193509, 2006.
[43] R. C. Smythe, "Intermodulation in thickness-shear resonators," in *28th Annu. Symp. on Frequency Control*, 1974, pp. 5–7.
[44] J. Nosek, "A critical evaluation of the determination of high-order elastic stiffnesses of quartz," in *IEEE Int. Frequency Control Symp. and PDA Exhibition*, 2001, pp. 324–328.
[45] H. P. Moyer, R. G. Nagele, R. L. Kubena, R. J. Joyce, D. J. Kirby, Y. Yong, P. D. Brewer, and D. T. Chang, "Nonlinear behavior of an UHF quartz resonator in an oscillating system," in *Proc. IEEE Int. Frequency Control Symp.* 2012, pp. 1–5.
[46] Y.-K. Yong, "A new nonlinear coupling of the fundamental and its harmonic overtone thickness shear modes for improvement of resonator Q," in *IEEE Ultrasonics Symp.*, 2012, pp. 170–173.
[47] J. J. Gagnepain, "Nonlinear constants and their significance," in *41st Annu. Symp. on Frequency Control*, 1987, pp. 266–276.
[48] H. F. Tiersten, "Nonlinear electroelastic equations cubic in the small field variables," *J. Acoust. Soc. Am.*, vol. 57, no. 3, pp. 660–666, 1975.
[49] P. C. Y. Lee, Y. S. Wang, and X. Markenscoff, "High-frequency vibrations of crystal plates under initial stresses," *J. Acoust. Soc. Am.*, vol. 57, no. 1, pp. 95–105, 1975.
[50] R. D. Mindlin, "High frequency vibrations of piezoelectric crystal plates," *Int. J. Solids Struct.*, vol. 8, no. 7, pp. 895–906, 1972.
[51] H. F. Tiersten and A. Ballato, "Nonlinear extensional vibrations of quartz rods," *J. Acoust. Soc. Am.*, vol. 73, no. 6, pp. 2022–2033, 1983.
[52] J. S. Yang and J. A. Kosinski, "Perturbation analysis of frequency shifts in an electroelastic body under biasing fields," *IEEE Trans. Ultrason. Ferroelectr. Freq. Control*, vol. 53, no. 12, pp. 2442–2449, 2006.

Authors' photographs and bios were unavailable at time of publication.